Biosensors and Bioelectronics 64 (2015) 462–468

Contents lists available at ScienceDirect

Biosensors and Bioelectronics

journal homepage: www.elsevier.com/locate/bios

A signal "on" photoelectrochemical biosensor for assay of protein kinase activity and its inhibitor based on graphite-like carbon nitride, Phos-tag and alkaline phosphatase

Huanshun Yin [a], Bing Sun [b], Linfeng Dong [a], Bingchen Li [a], Yunlei Zhou [a,*], Shiyun Ai [a,*]

[a] College of Chemistry and Material Science, Shandong Agricultural University, 271018 Taian, Shandong, PR China
[b] Key Laboratory of Molecular Nanostructure and Nanotechnology, Institute of Chemistry, Chinese Academy of Sciences (CAS), Beijing 100190, PR China

ARTICLE INFO

Article history:
Received 4 July 2014
Received in revised form
22 September 2014
Accepted 24 September 2014

Keywords:
Photoelectrochemical biosensor
Protein kinase activity
Graphite-like carbon nitride
Phos-tag
Inhibitor
Cell lysate

ABSTRACT

A highly sensitive and selective photoelectrochemical (PEC) biosensor is fabricated for the detection of protein kinase activity based on visible-light active graphite-like carbon nitride (g-C_3N_4) and the specific recognition utility of Phos-tag for protein kinase A (PKA)-induced phosphopeptides. For assembling the substrate peptides, g-C_3N_4 and gold nanoparticles (g-C_3N_4-AuNPs) complex is synthesized and characterized. When the immobilized peptides on g-C_3N_4–AuNPs modified ITO electrode are phosphorylated under PKA catalysis, they can be specifically identified and binded with biotin functionalized Phos-tag (Phos-tag–biotin) in the presence of Zn^{2+}. Then, through the specific interaction between biotin and avidin, avidin functionalized alkaline phosphatase (avidin-ALP) is further assembled to catalyze its substrate of L-ascorbic acid-2-phosphate trisodium salt (AAP) to produce electron donor of ascorbic acid (AA), resulting an increased photocurrent compared with the absence of phosphorylation event. Based on the specific identification effect of Phos-tag, the fabricated biosensor presents excellent selectivity for capturing the phosphorylated serine residues in the substrate peptides. With the good photoactivity of g-C_3N_4 and ALP-catalyzed signal amplification, the fabricated biosensor presents high sensitivity and low detection limit (0.015 unit/mL, $S/N=3$) for PKA. The applicability of this PEC biosensor is further testified by the evaluation of PKA inhibition by HA-1077 with the IC_{50} value of 1.18 μM. This new strategy is also successfully applied to detect the change of PKA activity in cancer cell lysate with and without drug stimulation. Therefore, the developed PEC method has great potential in screening of kinase inhibitors and highly sensitive detection of kinase activity.

1. Introduction

Photoelectrochemical (PEC) biosensor, as a kind of new detection technique, has attracted great interests because it contains the merits of electrochemical and optical assay (Hu et al., 2013; Wu et al., 2013; Zhang et al., 2011a). For the application of PEC biosensor, one of the crucial influence factors is photoactive material. Up to now, many kinds of photoactive materials have been investigated, such as organic photoelectronic materials, conducting polymer and inorganic semiconductor nanomaterials. Among them, the inorganic semiconductor nanomaterials have been widely investigated and applied in the fabrication of PEC biosensors, such as TiO_2, ZnO, WO_3, Bi_2S_3, BiOI, CdS, CdSe, ZnS, ZnZe, etc (Zhang et al., 2013b; Zhang and Zhao, 2013). Though these materials show great potential in PEC biosensor, there are several disadvantages. Initially, some materials have the wide band gap (such as TiO_2 and ZnO), which limits their applications in PEC biosensing since it can only absorbs UV light ($\lambda < 400$ nm) that can damage some biomolecules or destroy the detected biosystems (Kang et al., 2010). In order to overcome these shortcomings and broaden the adsorbed visible range, modification with narrow-band gap semiconductors or organic photosensitizer is necessary (Tu et al., 2010; Wang et al., 2009). But this modification will increase the experimental complexity. Secondly, most of these materials are metal-contained, which might be harmful to environment. Additionally, several materials only present weak photocurrent response and it might decrease the detection sensitivity when the signal "off" mode is selected. Therefore, the development of new photoactive material is necessary with the merits of fast photoelectronic response, easy preparation, nontoxicity and visible light activity.

Graphite-like carbon nitride (g-C_3N_4) is the most stable allotrope of carbon nitride and has recently attracted great interest

* Corresponding authors. Fax: +86 538 8242251.
E-mail addresses: zhyl@sdau.edu.cn (Y. Zhou), ashy@sdau.edu.cn (S. Ai).

http://dx.doi.org/10.1016/j.bios.2014.09.070
0956-5663/

because of its semiconductor properties and the advantages of easy preparation, simple instrument, cheap reagents, metal-free, visible-light response. So far, g-C_3N_4 has been widely used as photocatalyst and applied in the fields of catalysis (Wang et al., 2010; Zhang et al., 2013a), energy storage (Park et al., 2011), photoelectronic devices (Zhang et al., 2011b), optical sensors (Lee et al., 2011, 2012; Tian et al., 2013), electrochemiluminescent sensor (Chen et al., 2014; Li et al., 2014) and electrochemical sensor (Zhang et al., 2014). Recent research has indicated the potential application of g-C_3N_4 in PEC biosensor. For instances, Xu et al. (2013) developed a novel PEC strategy for the detection of Cu^{2+} with visible-light-driven AgX/g-C_3N_4 (X=Br, I) hybrid materials. Dai et al. (2014) fabricated a sensitive and highly efficient PEC biosensor for the quantitative detection of arecoline based on g-C_3N_4 nanosheets with the assistance of carbon nanohorns. Among these PEC biosensors, g-C_3N_4 and its compounds illustrated good PEC activity.

Protein phosphorylation, which is catalyzed by protein kinases, plays important roles in many biological processes involving cellular proliferation, gene transcription, cell growth and differentiation (Montminy, 1997). Aberrant expression of protein kinase has been associated with a series of diseases (Critchfield et al., 1997; Flajolet et al., 2007; Wang et al., 2001). Therefore, the identification of kinase and their potential inhibitors is not only necessary for basic biology to clarify molecular mechanisms of signal transduction but also valuable for protein kinase-targeted drug discovery and therapy. Therefore, simple, rapid and sensitive assays for determining specific protein kinase activity are needed to facilitate disease therapy and drug discovery.

For protein kinase activity assay, one of the key steps is the valid identification of phosphate group in peptide or protein. Until now, many recognition reagents have been developed, including ATP labeled with radioactive γ-^{32}P or ferrocene or –SH (Houseman et al., 2002; Kerman and Kraatz, 2007; Song et al., 2008), phosphorylated amino acid specific antibody (Shults et al., 2005), carboxypeptidase Y (Zhou et al., 2013), TiO_2 and Zr^{4+} (Bai et al., 2013; Chen et al., 2013), etc. Unfortunately, radioactive ATP suffers from complicated multi-steps operation, harmful to human health and radioactive pollution. Ferrocene or –SH labeled ATP presents complex synthetic process and expensive cost. The application of phosphorylated amino acid specific antibody is beset by the high cost, complicated preparation process, low binding force and the dependence of the type of amino acids (Kinoshita-Kikuta et al., 2009). TiO_2 and Zr^{4+} have the deficiency of low identification specificity.

For overcoming these defects, a kind of dinuclear metal complex that acts as a specific phosphate-binding agent, commercially known as Phos-tag, has been synthesized and applied to assay protein phosphorylation (Inamori et al., 2005; Kinoshita et al., 2006). In the presence of Zn^{2+} or Mn^{2+}, Phos-tag can form a specific noncovalent complex with the phosphomonoester dianion at neutral pH with excellent stability. More importantly, Phos-tag can specifically interact with phosphorylated peptides or proteins containing phospho-Serine, phospho-threonine, phospho-tyrosine, and phospho-histidine residues (Kinoshita et al., 2006; Yamada et al., 2007). Since the synthesis of Phos-tag, it has been widely applied in various techniques for assay and purification of phosphorylated proteins such as fluorescence, mass spectrometry, chromatography, surface plasmon resonance, western blot analysis and gel electrophoresis (Barbieri and Stock, 2008; Takiyama et al., 2009). To date, no reports have described methods for applying Phos-tag-based technologies to analyze the activity of protein kinase. We strived for the assay of kinase activity using Phos-tag and its derivatives. To this end, we developed a novel signal "on" PEC biosensor based on in situ enzymatic product of electron donor under visible-light irradiation, where g-C_3N_4 is used as photoactive material, biotin functionalized phos-tag (Phos-tag–biotin) as phosphate capture molecule and avidin functionalized alkaline phosphatase (avidin-ALP) as signal amplification unit.

2. Experimental section

2.1. Reagents and instruments

The substrate peptide (s-peptide, CGGALRRASLG), the control peptide (c-peptide, CGGALRRAALG), avidin-ALP and adenosine 5′-triphosphate (ATP) disodium salt hydrate are purchased from Sangon Biotech (Shanghai) Co., Ltd. cAMP-dependent protein kinase A (PKA) catalytic subunit, casein Kinase I (CK1), casein kinase II (CK2) and mitogen-activated protein kinase (MAPK) are purchased from New England Biolabs Ltd. (Beverly, MA). Phos-tag–biotin is obtained from Wako Pure Chemical Industries, Ltd. (Japan). 6-Mercapto-1-hexanol (MPH) is supplied by Sigma (USA). Tris(2-carboxyethyl) phosphine hydrochloride (TCEP), Tris (hydroxymethyl)aminomethane (Tris), chloroauric acid ($HAuCl_4$) and ascorbic acid (AA) are purchased from Aladdin (shanghai, China). L-Ascorbic acid-2-phosphate trisodium salt (AAP) is obtained from DiBo Chemical Technology co., Ltd. (Shanghai, China). HA-1077 is afforded by EMD Millipore Corporation (Billerica, MA, USA). ITO conductive glass is purchased from Zhuhai Kaivo Electronic Components Co., Ltd. (Zhuhai, China, ITO coating 180 ± 25 nm, sheet resistance $< 15\ \Omega/cm^2$). The buffer solutions and instruments applied in this work are listed in Supporting Informations.

2.2. Synthesis of g-C_3N_4 and g-C_3N_4–AuNPs nanohybrids

In a typical experiment, 3 g of dicyandiamide (99%) is placed in a ceramic boat and then loaded into the central region of a horizontal tube furnace. The tube furnace is heated to 220 °C at a heating rate of 3 °C/min and maintained at 220 °C for 2 h, and then the reactant is further heated to 350 and 550 °C and maintained at these temperatures for 2 and 4 h, respectively. Afterwards, the reaction system is allowed to cool to room temperature naturally. The product is dispersed in double distilled deionized water under ultrasonication and centrifuged at 12,000 rpm for three times to remove soluble reactants and impurities, and then washed three times with ethanol to remove some organic impurities. After drying at 60 °C, the obtained yellow product is ground into powder for further use.

g-C_3N_4–AuNPs nanohybrids are prepared according to previous report with some major modifications (Chen et al., 2014) (see Supporting Informations)

2.3. Biosensor fabrication

See Supporting information.

2.4. Cell culture and lysate preparation

Human hepatoma cell line HepG-2 and human hepatic cell line L-02 are cultured and lysated according to our previous report (Yin et al., 2015). And the operation process was described in Supporting information.

For stimulation, HepG-2 cells are first cultured with the process as described above. Then those cells are moved into a serum-free medium and cultured with another 4 h before simulation. Subsequently, forskolin and IBMX (dissolved in DMSO) solutions are added into the medium to activate intracellular PKA. For

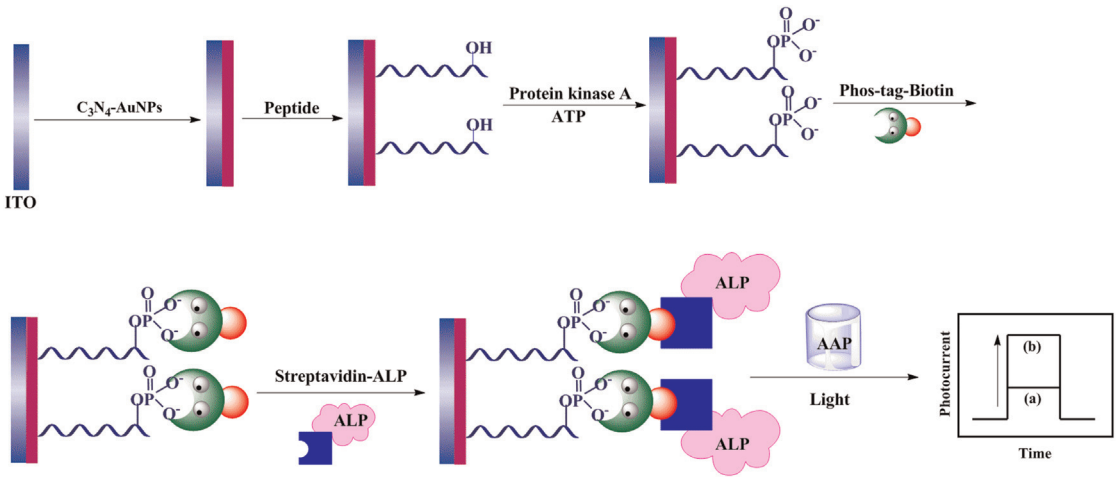

Scheme 1. Schematic diagram of the PEC biosensor construction process.

control, equal volume of DMSO is added into the medium for inactivated samples. Thirty minutes after stimulation, those cells are harvested and lysed as describe above. The obtained supernatants are stored at −80 °C in a refrigerator.

The total protein concentration in cell lysate is evaluated by modified Bradford protein assay kit according to the manufacturer's recommendation. All cell lysates are diluted to 10 μg/mL total protein concentration for kinase activity assay.

3. Results and discussion

3.1. Detection strategy

In this work, we develop a novel signal "on" PEC method for protein kinase activity assay based on in situ enzymatic generation of electron donor of AA and phosphate group recognition reagent of Phos-tag–biotin. As seen in Scheme 1, the substrate peptide is

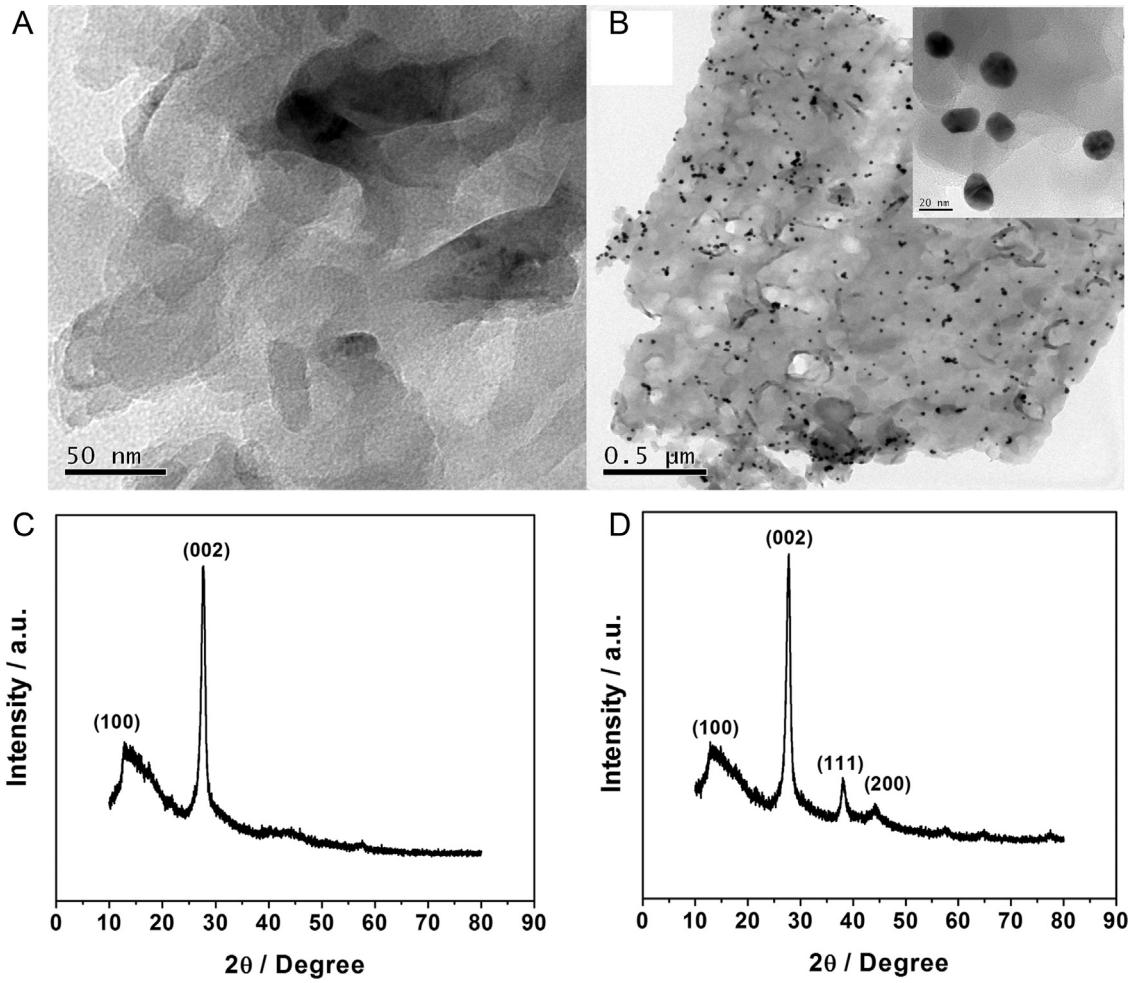

Fig. 1. TEM images of g-C_3N_4 (A) and g-C_3N_4–AuNPs complex (B). Inset of (B), HRTEM image of g-C_3N_4–AuNPs. XRD patterns of g-C_3N_4 (C) and g-C_3N_4–AuNPs complex (D).

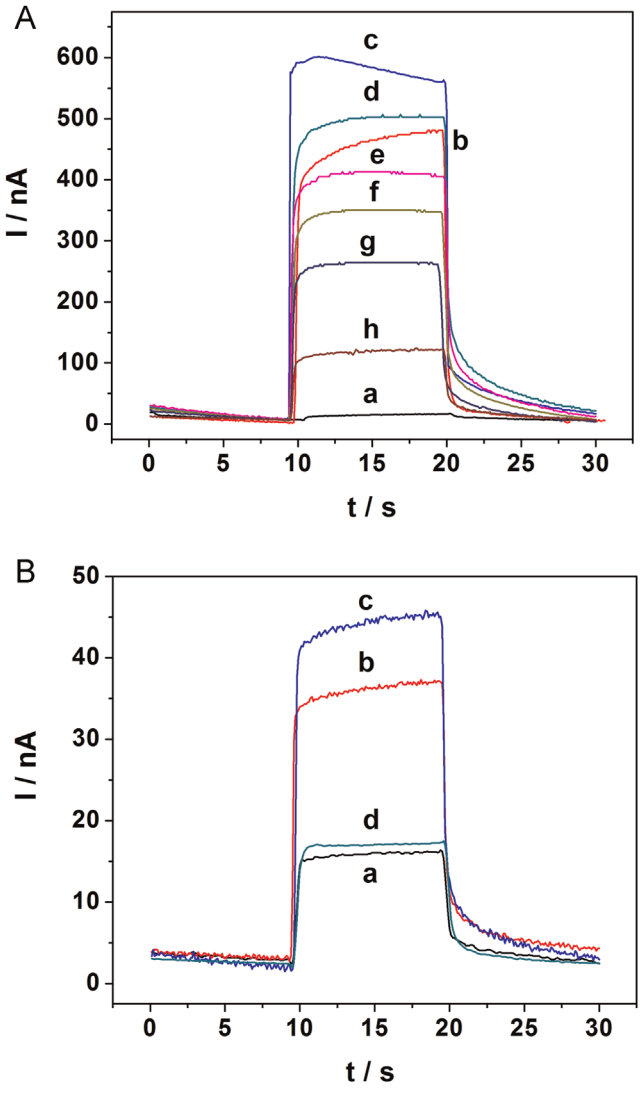

Fig. 2. (A) The photoelectrochemical response of different electrodes in 0.1 M PBS containing 0.1 M AA (pH 7.4). a: the bare ITO electrode; b: g-C_3N_4/ITO; c: AuNPs–g-C_3N_4/ITO; d: Peptide/AuNPs-g-C_3N_4/ITO; e: d after sealed with MPH; f: P-Peptide/AuNPs–g-C_3N_4/ITO; g: Phos-tag/P-Peptide/AuNPs–g-C_3N_4/ITO; h: ALP/Phos-tag/P-Peptide/AuNPs-g-C_3N_4/ITO. (B) The photoelectrochemical respose of different electrodes in 10 mM Tris–HCl (pH 9.8) containing 10 mM AAP and 0.1 mM Mg$(NO_3)_2$. a: Phos-tag/P-Peptide/g-C_3N_4–AuNPs/ITO; b and c: ALP/Phos-tag/P-Peptide/g-C_3N_4–AuNPs/ITO; d: Peptide/g-C_3N_4–AuNPs/ITO is directly treated with Phos-tag-biotin and avidin-ALP. The PKA concentration in b and c is 1 and 10 unit/mL, respectively.

firstly assembled on the g-C_3N_4–AuNPs/ITO electrode surface through the bonding effects between AuNPs and -SH, where the -SH is supplied by the cysteine residue at the C-terminal of the substrate peptide (H-CGGALRRASLG-NH_2). Then the serine residue in the sequence of ″LRRAS″ can be recognized and phosphorylated by PKA in the presence of ATP, where one phosphate group is transferred from ATP to serine residue. Subsequently, Phos-tag–biotin is selected as the identifying reagent for the phosphate group. Afterwards, the avidin-ALP is further captured on the electrode surface through the specific interaction between avidin and biotin. Finally, the immobilized ALP catalyzes its substrate of AAP to produce AA as electron donor, which can provide one electron to capture the photo-generated hole and decrease the recombination probability of photo-generated electron and hole of g-C_3N_4, resulting in an increased photocurrent. Through the relationship between the photocurrent and PKA concentration, the PKA can be detected. The novelty of this work is mainly located three aspects. The first is the photoactive material of g-C_3N_4. As a kind of “green” and visible light active material, the application of g-C_3N_4 can greatly decrease the environment hazards compared with other metal-contained photoactive materials. The second is Phos-tag–biotin, the derivative of the phosphate group recognition reagent of Phos-tag with high identification specificity. The third is in situ enzymatic generation of electron donor, resulting in a signal ″on″ detection mode.

3.2. Characterization of g-C_3N_4–AuNPs

The prepared g-C_3N_4–AuNPs is characterized by TEM and XRD. For comparison, the TEM and XRD for g-C_3N_4 are also performed. Fig. 1A showed the TEM image of the as-prepared pure g-C_3N_4 sample, revealing a clearly flat layer structure. For the TEM image for g-C_3N_4–AuNPs complex (Fig. 1B), lots of black dots are uniformly decorated on the g-C_3N_4 surface, indicating that the synthesized AuNPs with the diameter about 20 nm are tightly anchored on the g-C_3N_4 surface. The XRD patterns are presented in Fig. 1C and D. For the pure g-C_3N_4 product, a characteristic diffraction peak at 27.7°, corresponding to the (002) plane, is obtained, which is associated with the interplanar stacking of conjugated aromatic systems. After the reduction of $AuCl_4^{3-}$ and production of AuNPs on g-C_3N_4 surface, another two diffraction peaks are observed at 38.1° and 44.4°, which are the typical diffraction peaks for the (111) and (200) planes of AuNPs, respectively. These results further prove the successfully chemical reduction preparation of AuNPs on g-C_3N_4 surface.

3.3. Biosensors characterization and detection feasibility assay

For the characterization of the biosensor fabrication, the photocurrents of ITO electrode with different modification process are recorded and compared in 0.1 M PBS containing 0.1 M AA (detection buffer 1) under visible light irradiation. As shown in Fig. 2A, only a weak PEC signal is observed at the bare ITO electrode (curve a). After immobilization of g-C_3N_4, a strong photocurrent is observed (curve b), which is originated from g-C_3N_4, indicating the good photoactive of g-C_3N_4. Then, the photocurrent further enhances (curve c) when g-C_3N_4–AuNPs complex is used as photoactive material instead of g-C_3N_4, and this increase could be attributed to AuNPs, which facilitate the transfer of photo-generated electron to electrode surface. However, the photocurrent decreases (curve d) when the substrate peptide is assembled on the g-C_3N_4–AuNPs/ITO electrode surface. This decrease can be attributed to the steric-hindrance effect of peptide, which blocks the diffusion of AA to electrode surface to prohibit the recombination of photo-generated electron and hole of g-C_3N_4. The similar result is also obtained when g-C_3N_4–AuNPs/ITO is sealed with MCH (curve e). Subsequently, the photocurrent decreases sequentially after the Peptide/g-C_3N_4–AuNPs/ITO electrode is incubated with PKA reaction buffer solution containing 1 unit/mL of PKA for 40 min (curve f), which can be ascribed to the phosphorylation event appearing in serine residue of the substrate peptide. Based on phosphorylation, one phosphate group with two negative charges is transferred to serine residue from ATP. Consequently, the diffusion of AA is further hindered due to electrostatic repulsion effect between phosphate group and AA because AA ($pK_{a1}=4.1$) is controlled by negative charge in the detection buffer with pH 7.4 (Busbee et al., 2003). Afterwards, the photocurrent further decreases when the electrode is incubated with Phos-tag–biotin (curve g). Based on this decrease, two conclusions can be deduced. One is the successful phosphorylation reaction, and the other is the effective assembly of Phos-tag–biotin through its specific identification effect towards phosphate group. After the electrode is further immersed with avidin-ALP, a much low

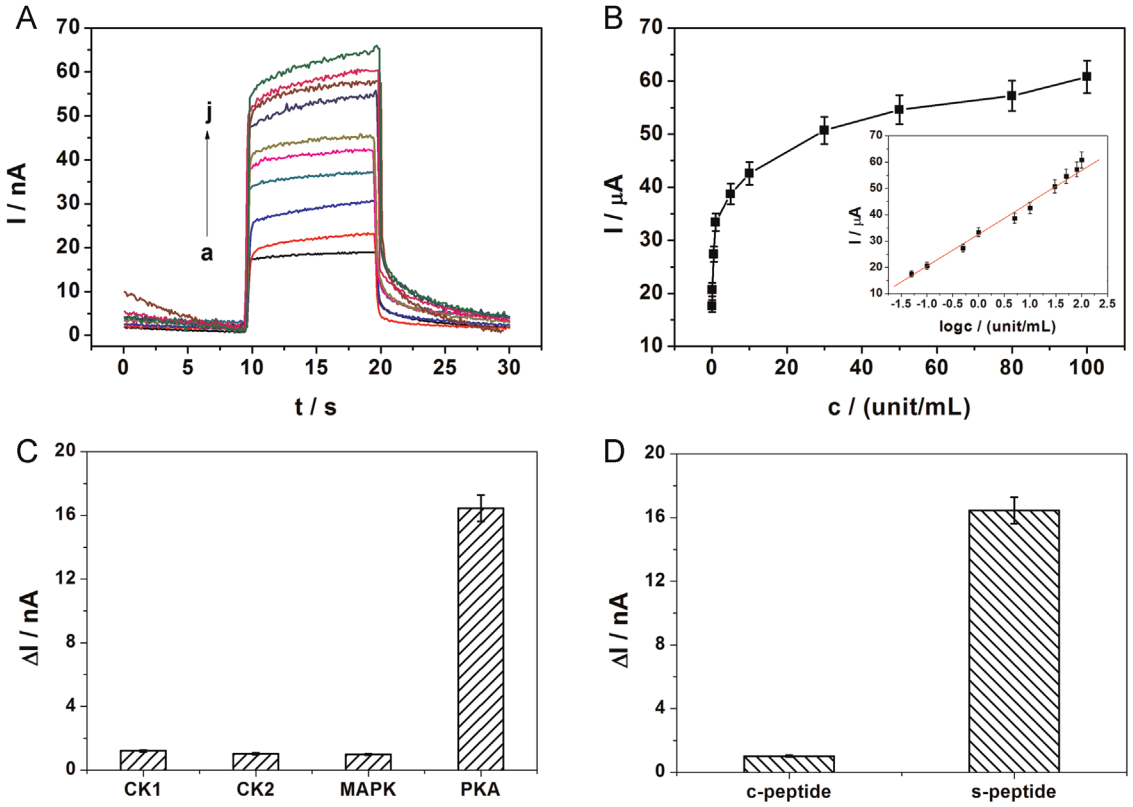

Fig. 3. (A) The photoelectrochemical response of the fabricated biosensor with different concentrations of PKA. a–j: 0.05, 0.1, 0.5, 1, 5, 10, 30, 50, 80, 100 unit/mL. (B) The plot for the concentration of PKA versus the photocurrent. Insert: Calibration curve. (C) The histogram for the photoelectrochemical response change of the biosensor incubated with different kinases. (D) The histogram for the photoelectrochemical response change of the biosensor with different peptide sequences.

photocurrent is obtained (curve h), which indicates the successful capture of avidin-ALP through the specific interaction between biotin and avidin. Through the photocurrent change of each modification step, the successful fabrication of the biosensor could be confirmed.

For testifying the detection feasibility of the fabricated biosensor for PKA activity based on ALP-catalytic signal amplification and in situ production of electron donor of AA, the photocurrents are also recorded in 10 mM Tris–HCl (pH 9.8) containing 10 mM AAP and 0.1 mM $Mg(NO_3)_2$ (detection buffer 2). As shown in Fig. 2B, only a weak photocurrent is observed for Phos-tag/P-Peptide/g-C_3N_4–AuNPs/ITO (curve a), which is caused by the lack of electron donor in the detection buffer 2. However, the photocurrent increases significantly after the detection buffer 2 is incubated with ALP/Phos-tag/P-Peptide/g-C_3N_4–AuNPs/ITO for 60 min (curve b). This increased photocurrent can be attributed the captured ALP, which catalyzes the hydrolysis reaction of AAP to produce the electron donor of AA. To further prove the detection feasibility, we increase the PKA concentration from 1 to 10 unit/mL. As expected, the photocurrent accordingly increased (curve c). It can be explained as the fact that the captured amount of ALP is increased with increasing PKA concentration, which results in an improved catalytic efficiency of ALP for the hydrolysis reaction and produces more electron donor of AA. As a result, the recombination probability for the electron and hole decreases greatly and the corresponding photocurrent increases.

In order to verify the importance of the phosphorylation event in the assay of PKA, we also compare the photocurrent change of Peptide/g-C_3N_4–AuNPs/ITO treated with PKA and without PKA. The results are also listed in Fig. 2B. When the Peptide/g-C_3N_4–AuNPs/ITO electrode is directly treated with Phos-tag–biotin and avidin-ALP (curve d), the fabricated biosensor only presents a weak photocurrent compared with ALP/Phos-tag/P-Peptide/g-C_3N_4–AuNPs/ITO. Without incubating with PKA, the serine residue can not be phosphorylated, which results in the failure of capture of Phos-tag–biotin and avidin-ALP. Consequently, the photocurrent is weak due to the absence of electron donor of AA in the detection buffer 2.

Based on the above researches, we believe that the developed method can be applied to analysis PKA activity.

3.4. PKA activity assay

Under optimum conditions (Fig. S1 in Supporting Information), with increasing the PKA concentration from 0.05 to 100 unit/mL, the photocurrent enhances gradually (Fig. 3A and B). As shown in the insert of Fig. 3B, the photocurrent is proportional to the logarithm value of PKA concentration in the range of 0.05–100 unit/mL with the linear regression equation of $I=12.11\log c+36.61$ ($R=0.9942$). The detection limit is estimated to be 0.17 unit/mL ($S/N=3$). The detection performance of our work is compared with some of previous reports. As listed in Table S1 (Supporting Information), though the detection limit of our work is a little higher than that at electrochemiluminescence (ECL), it is lower than most of other techniques, such as electrochemistry, fluorescence and quartz crystal microbalance (QCM). Thus, this method has good potential for protein kinase activity assay.

As a potentially applicable analysis method, it should possess not only low detection limit and wide linear range, but also excellent detection specificity and reproducibility. Therefore, for detecting the specificity and reproducibility, the peptide/g-C_3N_4–AuNPs/ITO is firstly incubated with other three protein kinases (such as CK1, CK2 and MAPK, 1 unit/mL, which can not recognize and phosphorylate the serine residue in the substrate peptide of CGGALRRASLG), respectively. Then the electrode is further incubated with Phos-tag–biotin and avidin-ALP successively. Finally,

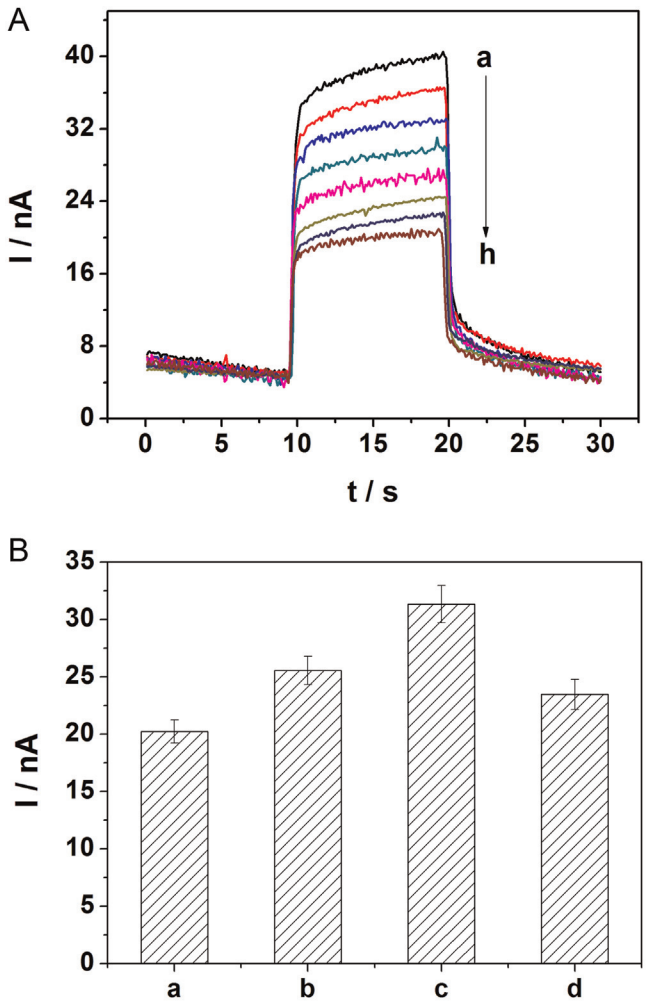

Fig. 4. (A) The photoelectrochemical response of the biosensor after PKA is inhibited with different concentrations of HA-1077. a–h: 0, 0.1, 0.5, 1, 1.5, 2, 3, 4 μM. (B) The histogram for the photocurrent of the biosensor incubated with PKA extracted from different cells. a: L-02 cells; b: HepG-2 cells; c: HepG-2 cells after stimulation with forskolin and IBMX; d: c inhibited with 1 μM HA-1077.

the photocurrent is recorded in detection buffer 2 and the photocurrent change ($\Delta I = I_1 - I_2$) is compared, where I_1 is the photocurrent of peptide/g-C_3N_4–AuNPs/ITO incubated with kinase, Phos-tag-biotin and avidin-ALP and I_2 is the photocurrent of peptide/g-C_3N_4–AuNPs/ITO. As can be seen in Fig. 3C, after the peptide/g-C_3N_4–AuNPs/ITO is incubated with other kinases, the ΔI is much lower than that obtained at PKA incubated peptide/g-C_3N_4–AuNPs/ITO, indicating acceptable detection specificity. For further proving the detection specificity, we also assemble the c-peptide on g-C_3N_4–AuNPs/ITO surface, and then incubated with PKA (1 unit/mL), Phos-tag–biotin and avidin-ALP successively. Due to the absence of correct peptide sequence, the phosphorylation event is not emerged, which leads to the failure of the following modification processes and a low ΔI (Fig. 3D). We also investigated some bioactive molecules on the effects of PKA detection. The results indicated that 0.1 μM ascorbic acid, 0.1 μM dopamine, 0.1 μM glucose and 1 unit/mL horseradish peroxidase, and 1 unit/mL tyrosinase do not influence PKA detection (The photocurrent change was lower than ±5%.) The reproducibility of the proposed method is evaluated by detecting 1 unit/mL of PKA using 10 independently fabricated biosensors. The relative standard deviation for ten determinations is 6.29%, indicating acceptable detection reproducibility.

3.5. Inhibition assay

The screening of small molecule inhibitors for protein kinase is of high importance in the discovery of kinase-targeted anti-cancer pharmaceuticals. To demonstrate the potential application of our method in protein kinase inhibitor screening, one potent PKA inhibitor, HA-1077, is selected as a model. As seen from Fig. 4A, with increasing concentration of HA-1077, the photocurrents decrease gradually, indicating a low activity of PKA and a low phosphorylation level. This result also proves the inhibition effects of HA-1077 on PKA activity. The relationship between the inhibition ratio and HA-1077 concentration is plotted in Fig. S2 (see Supporting information), from which the IC_{50} value (the half-maximal inhibitory concentration) is calculated to be 1.18 μM. These results clearly suggest that the proposed protocol is of great potential in screening protein kinase inhibitors.

3.6. Detection of PKA activity in cell lysates

The developed method is applied to analyze the PKA activity in the lysate of human hepatoma cell line HepG-2. As control, the PKA activity in the lysate of human hepatic cell line L-02 is also detected. For performing it, the Peptide/g-C_3N_4–AuNPs/ITO is first incubated with cell lysate, then with Phos-tag–biotin and avidin-ALP. Finally, the photocurrent is recorded in detection buffer 2 after incubation of 60 min. As seen in Fig. 4B, the photocurrent for HepG-2 cell lysate incubated electrode (column b) is higher than that obtained at L-02 cell lysate (column a), which demonstrates a high PKA activity in hepatoma cell lysate. It has been reported that the PKA activity can be efficiently up-regulated by the external activating reagents of forskolin and IBMX (Meggio et al., 1995; Zhou et al., 2013). Hence, for further verifying the applicability of our method for PKA activity assay in cytosolic environment, we activate PKA activities through adding 10 μM forskolin and 20 μM IBMX to stimulate HepG-2 cell for 30 min, and then the activated cells are lysated and the supernate is collected for detection. Subsequently, the Peptide/g-C_3N_4–AuNPs/ITO is incubated with lysate for phosphorylation, then with Phos-tag–biotin and avidin-ALP. Finally, the photocurrent is recorded and the PKA activity is evaluated according to the photocurrent change. As also shown in Fig. 4B, column c, the photocurrent increased after stimulation, indicating an enhanced PKA activity. In order to testify the origin of the PEC signal, the photocurrent is also recorded after inhibiting by HA-1077 (Fig. 4B, column d). The result presents a decreased PEC response, indicating that the increased photocurrent is directly originated from PKA activity based on stimulation. These results also demonstrate that our developed method can be efficiently applied to detect PKA activity in complex biological system.

4. Conclusion

In summary, a sensitive and selective PEC biosensor is fabricated for PKA activity assay and inhibitor screening, in which g-C_3N_4 is used as photoactive material, Phos-tag-biotin as phosphate identification element, and avidin-ALP as signal amplification unit. This PEC biosensor presents several distinct advantages. Firstly, the photoactive material of g-C_3N_4 is metal-free, which completely eliminates the risk of environmental pollution originated from metal-contained photoactive material. Moreover, the easy preparation and cheap reagents for g-C_3N_4 also facilitates the biosensor fabrication. Secondly, the photoactivity of g-C_3N_4 is greatly improved through the doping of AuNPs into g-C_3N_4 to form composite material. Thirdly, the Phos-tag-biotin presents extremely high selectivity for the identification and capture of

phosphate group in the substrate peptide, which also results in high detection sensitivity through the effective capture of avidin-ALP through the specific interaction between biotin and avidin. Moreover, under the catalytic effect of ALP towards AAP, the electron donor of AA is produced directly in the detection buffer solution, and based on it, the signal-on detection strategy is achieved. According to these advantages, the high sensitive and selective assay of protein kinase activity and inhibitor screening are testified. Furthermore, the developed method is also successfully applied to detect protein kinase activity in cell lysates, which illustrates the great potential for kinase-related drug discovery, early diagnosis of disease and evaluation of therapeutic efficacy.

Acknowledgements

This work is supported by the National Natural Science Foundation of China (nos. 21105056, 21375079), China Postdoctoral Science Foundation (2014M550369) and the Project of Development of Science and Technology of Shandong Province, China (no. 2013GZX20109).

Appendix A. Supporting information

Supplementary data associated with this article can be found in the online version at http://dx.doi.org/10.1016/j.bios.2014.09.070.

References

Bai, J., Zhao, Y., Wang, Z., Liu, C., Wang, Y., Li, Z., 2013. Anal. Chem. 85 (9), 4813–4821.
Barbieri, C.M., Stock, A.M., 2008. Anal. Biochem. 376 (1), 73–82.
Busbee, B.D., Obare, S.O., Murphy, C.J., 2003. Adv. Mater. 15 (5), 414–416.
Chen, L., Zeng, X., Si, P., Chen, Y., Chi, Y., Kim, D.-H., Chen, G., 2014. Anal. Chem. 86 (9), 4188–4195.
Chen, Z., He, X., Wang, Y., Wang, K., Du, Y., Yan, G., 2013. Biosens. Bioelectron. 41, 519–525.
Critchfield, J.W., Coligan, J.E., Folks, T.M., Butera, S.T., 1997. Proc. Natl. Acad. Sci. 94 (12), 6110–6115.
Dai, H., Zhang, S., Xu, G., Gong, L., Li, X., Zeng, C., Lu, S., Jiang, Y., Lin, Y., Chen, G., 2014. RSC Adv. 4 (22), 11099–11102.
Flajolet, M., He, G., Heiman, M., Lin, A., Nairn, A.C., Greengard, P., 2007. Proc. Natl. Acad. Sci. 104 (10), 4159–4164.
Houseman, B.T., Huh, J.H., Kron, S.J., Mrksich, M., 2002. Nat. Biotechnol. 20 (3), 270–274.
Hu, C., Zheng, J., Su, X., Wang, J., Wu, W., Hu, S., 2013. Anal. Chem. 85 (21), 10612–10619.
Inamori, K., Kyo, M., Nishiya, Y., Inoue, Y., Sonoda, T., Kinoshita, E., Koike, T., Katayama, Y., 2005. Anal. Chem. 77 (13), 3979–3985.
Kang, Q., Yang, L., Chen, Y., Luo, S., Wen, L., Cai, Q., Yao, S., 2010. Anal. Chem. 82 (23), 9749–9754.
Kerman, K., Kraatz, H.-B., 2007. Chem. Commun. 47, 5019–5021.
Kinoshita-Kikuta, E., Kinoshita, E., Koike, T., 2009. Anal. Chem. 389 (1), 83–85.
Kinoshita, E., Kinoshita-Kikuta, E., Takiyama, K., Koike, T., 2006. Mol. Cell. Proteomics 5 (4), 749–757.
Lee, E.Z., Jun, Y.-S., Hong, W.H., Thomas, A., Jin, M.M., 2011. Angew. Chem. Int. Ed. 49 (50), 9706–9710.
Lee, E.Z., Lee, S.U., Heo, N.-S., Stucky, G.D., Jun, Y.-S., Hong, W.H., 2012. Chem. Commun. 48 (33), 3942–3944.
Li, X., Zhang, X., Ma, H., Wu, D., Zhang, Y., Du, B., Wei, Q., 2014. Biosens. Bioelectron. 55, 330–336.
Meggio, F., Deana, A.D., Ruzzene, M., Brunati, A.M., Cesaro, L., Guerra, B., Meyer, T., Mett, H., Fabbro, D., Furet, P., 1995. Eur. J. Biochem. 234 (1), 317–322.
Montminy, M., 1997. Annu. Rev.Biochem. 66 (1), 807–822.
Park, S.S., Chu, S.-W., Xue, C., Zhao, D., Ha, C.-S., 2011. J. Mater. Chem. 21 (29), 10801–10807.
Shults, M.D., Janes, K.A., Lauffenburger, D.A., Imperiali, B., 2005. Nat. Methods 2 (4), 277–284.
Song, H., Kerman, K., Kraatz, H.-B., 2008. Chem. Commun. 4, 502–504.
Takiyama, K., Kinoshita, E., Kinoshita-Kikuta, E., Fujioka, Y., Kubo, Y., Koike, T., 2009. Anal. Biochem. 388 (2), 235–241.
Tian, J., Liu, Q., Asiri, A.M., Al-Youbi, A.O., Sun, X., 2013. Anal. Chem. 85 (11), 5595–5599.
Tu, W., Dong, Y., Lei, J., Ju, H., 2010. Anal. Chem. 82 (20), 8711–8716.
Wang, G.-L., Xu, J.-J., Chen, H.-Y., 2009. Biosens. Bioelectron. 24 (8), 2494–2498.
Wang, H., Davis, A., Yu, S., Ahmed, K., 2001. Mol. Cell. Biochem. 227 (1-2), 167–174.
Wang, Y., Zhang, J., Wang, X., Antonietti, M., Li, H., 2010. Angew. Chem. Int. Ed. 49 (19), 3356–3359.
Wu, Y., Zhang, B., Guo, L.-H., 2013. Anal. Chem. 85 (14), 6908–6914.
Xu, L., Xia, J., Xu, H., Qian, J., Yan, J., Wang, L., Wang, K., Li, H., 2013. Analyst 138 (22), 6721–6726.
Yamada, S., Nakamura, H., Kinoshita, E., Kinoshita-Kikuta, E., Koike, T., Shiro, Y., 2007. Anal. Biochem. 360 (1), 160–162.
Yin, H., Wang, M., Li, B., Yang, Z., Zhou, Y., Ai, S., 2015. Biosens. Bioelectron. 63, 26–32.
Zhang, H., Huang, Q., Huang, Y., Li, F., Zhang, W., Wei, C., Chen, J., Dai, P., Huang, L., Huang, Z., Kang, L., Hu, S., Hao, A., 2014. Electrochim. Acta , http://dx.doi.org/10.1016/j.electacta.2014.1007.1094.
Zhang, J., Wang, Y., Jin, J., Zhang, J., Lin, Z., Huang, F., Yu, J., 2013a. ACS Appl. Mater. Interfaces 5 (20), 10317–10324.
Zhang, X., Guo, Y., Liu, M., Zhang, S., 2013b. RSC Adv. 3 (9), 2846–2857.
Zhang, X., Li, S., Jin, X., Zhang, S., 2011a. Chem. Commun. 47 (17), 4929–4931.
Zhang, Y., Mori, T., Niu, L., Ye, J., 2011b. Energy Environ. Sci. 4 (11), 4517–4521.
Zhang, Z.-X., Zhao, C.-Z., 2013. Chin. J. Analy. Chem. 41 (3), 436–444.
Zhou, J., Xu, X., Liu, W., Liu, X., Nie, Z., Qing, M., Nie, L., Yao, S., 2013. Anal. Chem. 85 (12), 5746–5754.